GAUSSIAN AND CRITICAL SCALINGS IN THE MAGNETOCONDUCTIVITY FLUCTUATIONS OF $Y_3BA_5CU_8O_{18}$ SUPERCONDUCTOR⋆

F. T. Dias[*,†], V. N. Vieira[*], C. P. Oliveira[*], D. L. Silva[*], F. Mesquita[*] and J. R. Lima[*]

[*]*Instituto de Física e Matemática, Universidade Federal de Pelotas, Caixa Postal 354, Pelotas, 96010-900, Rio Grande do Sul, Brazil*[‡]
fabio.dias@ufpel.edu.br[§]

F. Wolff-Fabris[+] and E. Kampert[+]

[+]*Dresden High Magnetic Field Laboratory, Helmholtz-Zentrum Dresden-Rossendorf, Dresden, 01314, Germany*

P. Pureur[++]

[++]*Instituto de Física, Universidade Federal do Rio Grande do Sul, Porto Alegre, 91501-970, Rio Grande do Sul, Brazil*

Received Day Month Day
Revised Day Month Day

We have studied the superconducting transition and the magnetoconductivity fluctuations in the polycrystalline $Y_3Ba_5Cu_8O_{18}$ (Y358) superconductor under magnetic fields up to 1 T. A two-step superconducting transition could be observed as a consequence of the granular structure of the sample, which is strongly affected by the applied magnetic field. Gaussian and genuine critical 3D-XY-E fluctuation regimes were identified. A critical scaling regime beyond 3D-XY was identified for magnetic fields up to 0.25 T, corresponding to the averaged exponent 0.19 and suggesting the occurrence of the weak first-order character of the superconducting transition. In the approximation to the zero resistance a power law regime could be observed, corresponding to the averaged exponent 2.37, who are smaller than previously reported for the Y358 system. Our results are discussed in terms of the Y358 and $YBa_2Cu_3O_{7-\delta}$ (Y123) results in the literature.

Keywords: Magnetoconductivity fluctuations; $Y_3Ba_5Cu_8O_{18}$ superconductor; Gaussian and critical exponents.

1. Introduction

The discovery of the high temperature $YBa_2Cu_3O_{7-\delta}$ (Y123) superconductor in 1986 by Müller and Bednorz[1] was the starting point in the YBaCuO-family. Other members were discovered along the subsequent years, among them the $Y_3Ba_5Cu_8O_{18}$ (Y358) superconductor by Aliabadi *et al*.[2] The Y358 allowed access a new phenomenology among the superconducting cuprates, and

[†]Corresponding author.
[‡]State completely without abbreviations, the affiliation and mailing address, including country. Typeset in 8 pt Times Italic.
[§]Typeset author e-mail address in single line.

several studies have been carried out in order to investigate the properties of this compound since then.

There are many differences among the YBaCuO-family members. For example, the Y123, the most known investigated member, has a structure constituted by two CuO_2 planes and one CuO chain, while the Y358 has five CuO_2 planes and three CuO chains. As a consequence, different aspects of the physical and superconducting properties can be observed, such as the temperature dependence of electric resistance,[3] the critical temperature (T_C),[3,4] and the magnetic irreversibility,[5] for example. The Y358 may be synthesized by different techniques, including sol-gel[6,7] and biopolymer routes,[8] resulting in sintered,[9-11] melt-textured,[12] nanowires and nanorods[8] samples.

There are few results involving a detailed study of thermodynamic fluctuations in the superconducting transition of the Y358 superconductor,[4,13] in spite of the large number of such results that can be found for the Y123 superconductor.[14-18] Such results are very interesting, and can provide relevant information on the mesoscopic morphology nature of the superconducting transition on cuprates, which is still quite controversial.

In this work we present a study on the thermodynamic fluctuations in the magnetoconductivity of the polycrystalline Y358 under magnetic fields up to 1 T. This study consists in a detailed investigation of the superconducting transition near T_C, where the occurrence of Gaussian and critical fluctuation regimes were identified by scaling laws. The experimental results are discussed based on the predictions of the 3D-XY-E universality class[19] and in comparison with the Y123 superconductor.

2. Experimental Details

2.1. *Sample preparation and structural characterization*

The Y358 sample was grown by standard solid-state reaction, starting from powders of Y_2O_3, $BaCO_3$ and CuO (Sigma-Aldrich, 99.999%) mixed according to the suitable stoichiometric ratio. After the mixed powders were calcined three times in air at 930 ºC for 12 h. In the next step the powders were pressed in a pellet of 10 mm in diameter and 2.5 mm of thickness under isostatic pressure. The pellet was sintered at 930 ºC for 24 h and annealed under a constant oxygen flow. After the sintering process the sample was previously analyzed by magnetic and electric techniques in order to verify the superconducting state. Finally the sample was cut in a small polycrystalline parallelepiped (1.31 x 1.79 x 4.66 mm^3) to perform the magnetoconductivity measurements.

The characterization was performed by scanning electron microscopy (SEM) and energy dispersive spectroscopy (EDS) techniques using a JSM-6390LV microscope from JEOL. The characterization results by X-ray diffraction, using a PANalytical XPert Pro MPD diffractometer, can be seen in the Ref. 5. Figs. 1(a) and 1(b) show SEM representative images of our sample, where the granular character can be evidenced, typical of sintered ceramic samples, with a disordered grain structure having an average size of few microns. Fig. 1(c) shows EDS results indicating the presence of the expected elements.

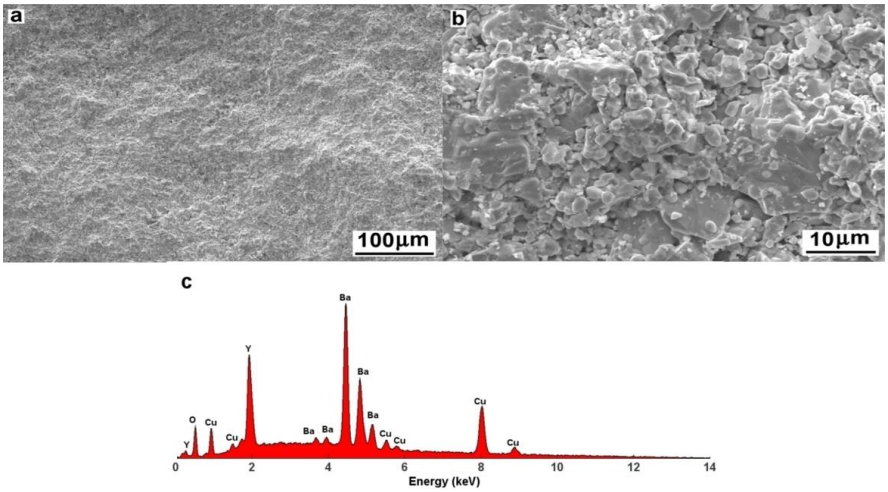

Fig. 1. (a) SEM image of the sample showing the granular structure typical of a sintered material. (b) SEM image showing details of the disordered grain structure. (c) EDS results confirming the expected elements.

2.2. *Magnetoconductivity measurements*

The magnetoconductivity measurements were performed in a PPMS (Physical Properties Measurements Systems) from Quantum Design, employing the four-contact technique under magnetic fields from 0 up to 1 T, with a DC current of 1 mA. In all measurements the magnetic field was applied parallel to the current direction in order to minimize the Lorentz force of the measuring current on the magnetic fluxons. However, in polycrystalline samples the flow of the electric current through the grains is highly dispersive and therefore this current/field configuration is microscopically only an approximation.

The Fig. 2 shows the temperature dependence of the resistivity, ρ (T), at zero applied field. The sample exhibits a metallic-like behavior along the normal state, followed by a transition to the superconducting state (zero resistivity). The normal state can be represented by a linear function such as

$$\rho(T) = \rho_0 + \alpha T, \qquad (1)$$

where ρ_0 is the residual resistivity and α is the resistivity temperature coefficient. In our sample such behavior is represented by the straight line in the Fig. 2, where the estimated values were ρ_0 = 1.27 mΩ.cm and α = 3.59 µΩ.cm/K. The insets show details of the temperature dependence of the resistivity near the superconducting transition and the temperature derivative of the resistivity, dρ/dT, where a two steps character of the transition can be clearly seen.

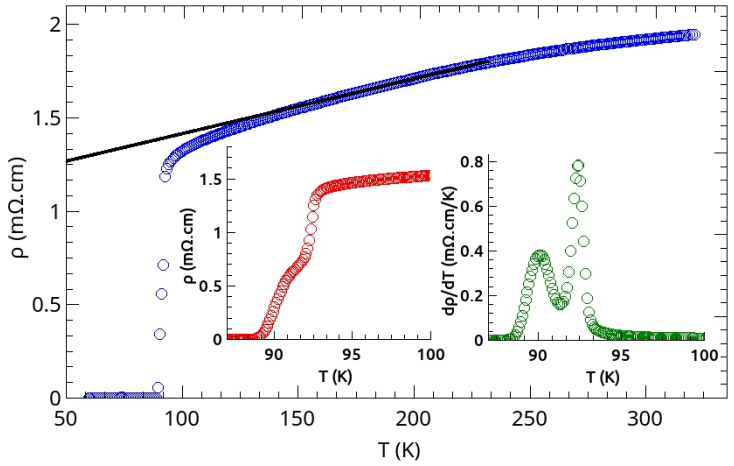

Fig. 2. The temperature dependence of the resistivity at zero magnetic field, where a metallic-like behavior can be observed. The insets show details of the two steps character of the superconducting transition.

3. Results and discussion

3.1. *Superconducting transition and dρ/dT*

The Fig. 3 shows the magnetoconductivity results obtained for magnetic fields ranging from 0 to 1 T. It is clear the broadening of the superconducting transition produced by the applied magnetic field, promoting a strong reduction in the zero resistivity temperature. This behavior is typical of polycrystalline samples, where granular effects are dominating. As reported in a previous work,[5] our polycrystalline sample displays strong granular behavior, as verified by the presence of Almeida-Thouless and Gabay-Toulouse regimes in a magnetic irreversibility study. In granular samples the electrical resistivity disappears just when the grain coupling leads to the long range coherence of the order parameter that percolates through the entire sample. Therefore, the electrical resistivity is controlled by grain junctions (Josephson junctions), vanishing when a long-range coherence is achieved. On the other hand, an external magnetic field can destroy the critical current along such junctions, resulting in an electrical resistance.

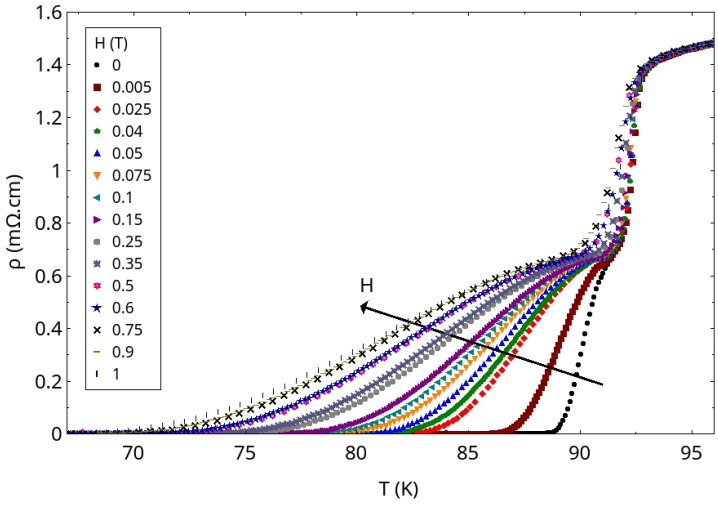

Fig. 3. Magnetoconductivity results for applied magnetic fields from 0 up to 1 T. The strong broadening in the transition produced by the magnetic field is a typical signature of granular effects.

Inspecting the Fig. 3, a two steps transition is evidenced, however, this feature can be seen more clearly by the respective temperature derivatives dρ/dT, represented by the panels of the Fig. 4 for different magnetic field ranges. The main peak (higher temperature) is slightly affected by the applied magnetic field, as can be seen comparing the three panels in the Fig. 4. The peak at higher temperatures denotes the pairing critical temperature T_P, as indicated in the inset of the panel (a). The peak at lower temperatures is strongly affected by the applied magnetic field and constitutes a characteristic signature of granular superconductors,[20-22] in which several superconducting grains are connected by weak links. This is a thermally controlled percolation process, dependent on meso and macroscopic inhomogeneities.[23,24] In such case the pairing transition stabilizes the superconductivity into the grains and at a lower temperature T_0 (see inset) a long-range coherent state is obtained, resulting in a zero electric resistivity. By comparing panels (a) and (c) for H = 0 and H = 1 T, respectively, is remarkable the strong broadening promoted by the magnetic field, where the difference in T_0 is higher than 20 K. The results for T_P and T_0 are summarized in Table 1.

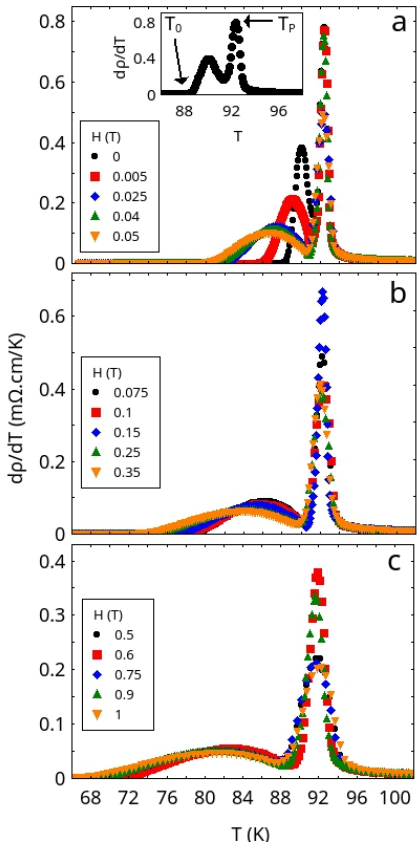

Fig. 4. The temperature derivatives dρ/dT for different magnetic field ranges, where the two steps transition can be seen in details. The inset in the panel (a) shows the pairing critical temperature T_P and the temperature where the zero electric resistivity is obtained, labeled by T_0. Comparing the panels (a), (b) and (c), the T_P values are slightly affected by the magnetic field, whereas the T_0 values are strongly affected, evidencing the granular characteristic of our sample, with superconducting grains connected by weak links.

3.2. *Superconducting fluctuations*

3.2.1. *Method of analysis*

Thermodynamic fluctuations on conductivity can create Cooper pairs above T_C. This process originates an excess of conductivity, sometimes called paraconductivity and represented by $\Delta\sigma$. Our experimental data were analyzed starting from the approach that the paraconductivity diverges as a power law given by

$$\Delta\sigma = A\varepsilon^{-\lambda}, \qquad (2)$$

where A is a constant, $\varepsilon = (T - T_C) / T_C$ is the reduced temperature, and λ is the critical exponent.

Table 1. Results for T_P and T_0 for each applied magnetic field.

H (T)	T_p (K)	T_0 (K)
0	92.44	87.94
0.005	92.35	85.34
0.025	92.28	81.26
0.04	92.32	80.43
0.05	92.29	79.69
0.075	92.28	78.29
0.1	92.36	77.60
0.15	92.23	76.63
0.25	92.10	74.36
0.35	92.05	72.66
0.5	91.72	70.62
0.6	91.85	69.66
0.75	91.72	68.63
0.9	91.65	68.05
1	92.25	66.82
Average	92.13	-

The paraconductivity $\Delta\sigma$ is given by $\sigma - \sigma_R$, where σ is the measured conductivity, and σ_R is the regular conductivity obtained by the extrapolation of the high temperature behavior of the resistivity curve, according to Eq. (1).

In order to obtain λ and T_C from Eq. (2), we determine numerically the logarithmic derivative of $\Delta\sigma$ from the experimental data, defining

$$\chi_\sigma = \frac{-d}{dT}\ln(\Delta\sigma). \quad (3)$$

Combining (2) and (3) we obtain

$$\frac{1}{\chi_\sigma} = \frac{1}{\lambda}(T - T_C), \quad (4)$$

which is analogous to a Curie-Weiss susceptibility in a ferromagnet, where the critical exponent λ plays the role of the Curie constant in this case. Consequently, based on a simple identification it is possible to extract simultaneously λ and T_C in plots of χ^{-1} versus T. This method has the simplicity as an advantage, however, there are some numerical uncertainties associated with it.[14]

By this method, five different exponents could be identified in our results and the Fig. 5 is a representative plot of χ^{-1} versus T at zero magnetic field. In the Fig. 5 the straight lines correspond to fits with Eq. (4), where the respective exponents, λ_{2D}, λ_{3D}, λ_C, λ_{SC} and S_0 are indicated. The temperatures T_C^C, T_C^G and T_{C0} were obtained by extrapolation of the regimes λ_{SC} (or λ_C), λ_{3D} and S_0, respectively. T_P indicates the pairing critical temperature, as for Fig. 4. From Fig. 5 it is evident that the superconducting transition is a two-step process, as pointed from Figs. 3 and 4. More details will be presented and discussed in the upcoming sessions.

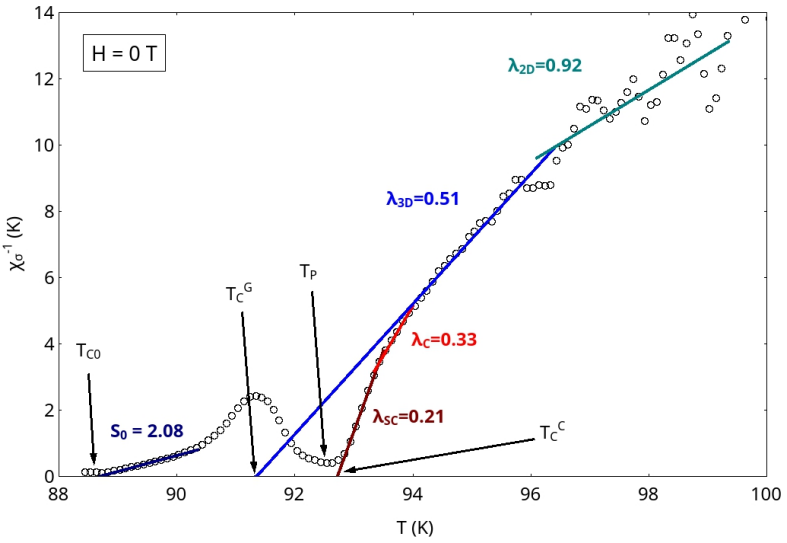

Fig. 5. Representative plot of χ^{-1} versus T showing the five different exponents identified according to our analysis, with the respective values at zero magnetic field. The temperatures T_C^C, T_C^G and T_{C0} were obtained by extrapolation of the regimes λ_{SC} (or λ_C, see the text), λ_{3D} and S_0, respectively. T_P is the pairing critical temperature (see Fig. 4).

3.2.2. *Gaussian fluctuations*

In the Fig. 5 the exponents labeled by λ_{2D} and λ_{3D} are representative of 2D and 3D Gaussian regimes, respectively. The 1D Gaussian regime could not be observed due to experimental uncertainty. The Fig. 6 shows results obtained from applied magnetic fields of 0.005, 0.04, 0.15, 0.35, 0.5 and 1 T, where the temperature T_C^G is indicated for each magnetic field. The regime λ_{2D} is most affected by experimental errors, as can be seen in the Fig. 6. By performing averages over all measurements (not shown here) we achieved $\lambda_{3D} = 0.51 \pm 0.01$, $\lambda_{2D} = 0.98 \pm 0.02$, and $T_C^G = (91.36 \pm 0.04)$ K.

Apparently the results showed in the Fig. 6 are in according to the Aslamazov-Larkin (AL) theory for fluctuation conductivity,[25] where the exponents are given by

$$\lambda = 2 - \frac{d}{2}, \tag{5}$$

and d is the dimensionality of the fluctuation regime. On the other hand, some of our exponents could not be explained by this model, once they do not correspond to integer dimensionality. However, by the assumption that the fluctuations develop in a space containing a fractal topology, as shown by Char and Kapitulnik,[26] the conductivity exponents are given by

$$\lambda = 2 - \frac{\bar{d}}{2}, \tag{6}$$

where $\bar{d}$is the respective fractal dimension of the superconducting aggregate.

Table 2. 2D and 3D Gaussian regimes observed in our sample, represented by the exponents λ_{2D} *and* λ_{3D}, *with the respective* Gaussian amplitudes A_{2D} and A_{3D}. ε is the reduced temperature indicating the range of validity of each regime and the temperature T_C^G is extrapolated from λ_{3D}, as shown in the Figs. 5 and 6. The exponent $\lambda_{3D\leftrightarrow 2D}$ is related to the fractal character of the superconducting fluctuations (see the text).

H (T)	λ_{3D} $0.0282 \leq \varepsilon \leq 0.0662$	$\lambda_{3D\leftrightarrow 2D}$ $0.0464 \leq \varepsilon \leq 0.0699$	λ_{2D} $0.0482 \leq \varepsilon \leq 0.1188$	A_{3D} $(m\Omega.cm)^{-1}$	A_{2D} $(m\Omega.cm)^{-1}$	T_C^G (K)
0	0.51	-	0.92	0.0118	0.0039	91.35
0.005	0.52	-	0.98	0.0116	0.0037	91.26
0.025	0.51	0.72	1.00	0.0119	0.0035	91.25
0.04	0.49	-	0.96	0.0121	0.0037	91.52
0.05	0.54	0.80	0.99	0.0111	0.0036	91.11
0.075	0.51	-	0.97	0.0118	0.0039	91.34
0.1	0.51	0.70	0.98	0.0117	0.0037	91.37
0.15	0.54	-	1.00	0.0108	0.0035	91.19
0.25	0.51	0.83	1.01	0.0117	0.0031	91.33
0.35	0.50	-	0.96	0.0118	0.0034	91.56
0.5	0.52	-	0.97	0.0116	0.0030	91.46
0.6	0.51	0.76	1.01	0.0114	0.0033	91.41
0.75	0.52	0.71	0.99	0.0111	0.0036	91.48
0.9	0.52	-	0.98	0.0115	0.0032	91.20
1	0.49	-	0.96	0.0121	0.0036	91.61
Average	0.51 ± 0.01	0.74 ± 0.05	0.98 ± 0.02	0.0116 ± 0.0004	0.0035 ± 0.0003	91.36 ± 0.04

The fractal character of the superconducting fluctuations have been reported in the Y123 superconductor in previous works,[14,24,27] but not for Y358 superconductor. This fractal regime is described by the exponent $\lambda_{3D\leftrightarrow 2D} = 0.74 \pm 0.05$. The Table 2 summarize the Gaussian regimes observed in our sample for all measurements, where ε is the reduced temperature indicating the range of validity of each fluctuation regime.

Another interesting result concerning Gaussian fluctuations is the persistence of the regime λ_{3D} for magnetic fields as high as 1 T, as can be seen in the Fig. 6, with no tendency to decrease for the applied magnetic field range. Previous results reported on Y123 show a robust λ_{3D} regime that remains even up 7 T, however is suppressed for the Y358 when magnetic fields above 1 T are applied.[13] Our results apparently are showing that the λ_{3D} regime could persist beyond 10 kOe. The Table 2 also shows the temperature T_C^G, extrapolated from λ_{3D}, which is practically invariant against the applied magnetic field, reinforcing the strength of the 3D Gaussian regime.

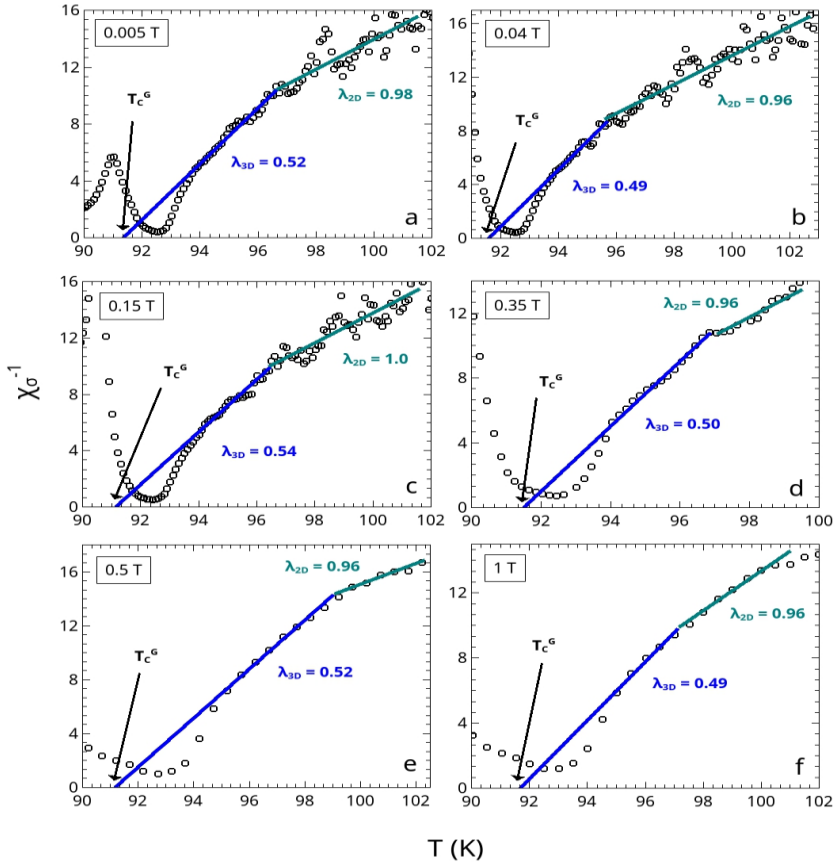

Fig. 6. Plots of χ^{-1} versus T for (a) 0.005, (b) 0.04, (c) 0.15, (d) 0.35, (e) 0.5 and (f) 1 T, showing Gaussian fluctuations regimes represented by the exponents λ_{2D} and λ_{3D}. The temperature T_C^G is indicated for each magnetic field.

According to the AL theory, the 2D and 3D Gaussian fluctuations have a critical amplitude given by

$$A_{2D} = \frac{e^2}{16\hbar d}, \tag{7}$$

and

$$A_{3D} = \frac{e^2}{32\hbar\xi(0)}, \tag{8}$$

respectively, where d is the relevant layer thickness for 2D fluctuations, and $\xi(0)$ is interpreted as the coherence length perpendicular to the layered structure, $\xi_C(0)$. In our results d and $\xi(0)$ could not be obtained with acceptable accuracy due to uncertainty related to the geometric factor of our sample. The Table 2 shows the respective Gaussian amplitudes obtained from the experiments, where it is possible to observe the absence of any systematic variation with the applied magnetic field.

3.2.3. *Critical fluctuations*

In the Fig. 5 the exponent labeled by λ_C corresponds to genuine critical fluctuations. In this case the critical exponent is given by

$$\lambda_C = \nu(2 + z - d + \eta), \tag{9}$$

where ν is the coherence length critical exponent, z is the dynamical critical exponent, d is the system dimensionality, and η is the exponent associated with the order parameter correlation function. Starting from 3D-XY model, renormalization-group calculations give $\nu \approx 0.67$ and $\eta \approx 0$.[29] Based on the model-E theory by Hohenberg and Halperin,[30] which predicts $z \approx 1.5$, the critical exponent λ_C has the value 0.33 for fluctuations conductivity. The 3D-XY-E scaling has been previously observed in polycrystalline,[14] single crystalline[31,32] and melt-textured[33] Y123 samples, and also in Y358 system.[11,13] The Fig. 7 shows results of genuine critical fluctuations represented by the critical exponent λ_C. In the same Fig. the 3D-Gaussian exponent λ_{3D} is also shown by the dashed line.

In spite of critical fluctuations have been observed in previous works with Y358 samples,[4,13] our results clearly show the persistence of the critical regime even for magnetic fields of 1 T, without apparent tendency of suppression. The strength of the critical regime against the applied magnetic field is not common even for single crystalline Y123 samples,[32] indicating a possible specific feature of the Y358 superconductor. The Table 3 shows the values obtained for the λ_C exponent, where ε is the reduced temperature. The Table 3 also shows the respective amplitude for the critical fluctuations, designated by A_C and according to the AL theory. Similar to the Gaussian regimes, it is possible to observe the absence of systematic variation with the magnetic field. As can be seen in the Figs. 7(d), (e) and (f), and summarized in the Table 3, T_C^C is the critical temperature extrapolated from the critical regime λ_C. The extrapolation of this fitting to the temperature axis allows a better evaluation of the pairing critical temperature.

Inspecting again the Fig. (7), more specifically the panels (a), (b) and (c), and also the Fig. 5, we can observe another critical regime named by λ_{SC}. The asymptotic critical regime, as can be seen also in the Table 3 with its respective amplitude A_{SC}, is present from zero up to 0.25 T, having an average value of 0.19 ± 0.03. This regime was first observed in an Y123 single crystal[31] and confirmed by further works,[16,32-34] including different superconducting cuprates.[35] The origin of such regime beyond 3D-XY-E is not totally known, however, according to the authors[31] it might be indicating that the ultimate character of the superconducting transition in cuprates is weakly first-order. Our results can be confirming and extending this characteristic to the Y358 system. On the other hand, the results in the Fig. 7 show that this scaling reaches the 3D-XY-E value when the magnetic field is higher than 0.25 T, according to the panels (d), (e) and (f). Such characteristic is not present in the Y123 system, where this regime is observed for magnetic fields well below 0.25 T.

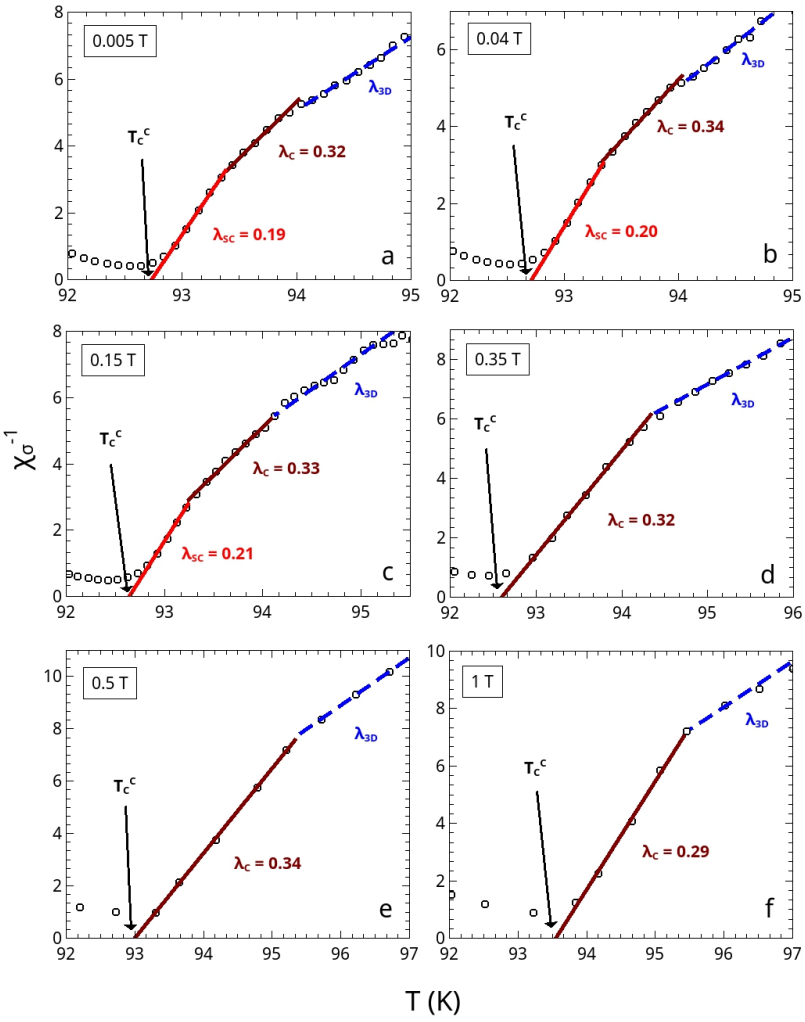

Fig. 7. Plots of χ^{-1} versus T for (a) 0.005, (b) 0.04, (c) 0.15, (d) 0.35, (e) 0.5 and (f) 1 T, showing critical fluctuations regimes represented by the exponents λ_C and λ_{SC}. The Gaussian regime λ_{3D} is also shown by the dashed line. The critical temperature T_C^C is indicated for each magnetic field

3.2.4. *Fluctuations near the zero resistance state*

Below the pairing critical temperature T_P, in the coherent region, the conductivity fluctuations diverge obeying the power law[20] given by

$$\Delta\sigma = A_0\varepsilon^{-S_0}, \qquad (10)$$

where A_0 is a constant, $\varepsilon = (T - T_{C0}) / T_{C0}$ is the reduced temperature, and S_0 is the critical exponent.

Table 3. Genuine critical fluctuations, represented by the exponents λ_{SC} *and* λ_C*, with the respective critical* amplitudes A_{SC} and A_C. ε is the reduced temperature and T_C^C is the critical temperature extrapolated from the critical regimes λ_{SC} and λ_C (see the text).

H (T)	λ_{SC} $0.0011 \leq \varepsilon \leq 0.0089$	λ_C $0.0053 \leq \varepsilon \leq 0.0213$	A_{SC} $(m\Omega.cm)^{-1}$	A_C $(m\Omega.cm)^{-1}$	T_C^C
0	0.21	0.33	0.0287	0.0169	92.72
0.005	0.19	0.32	0.0318	0.0177	92.75
0.025	0.18	0.35	0.0311	0.0151	92.98
0.04	0.20	0.34	0.0293	0.0160	92.75
0.05	0.20	0.33	0.0283	0.0165	92.92
0.075	0.19	0.33	0.0292	0.0160	92.97
0.1	0.17	0.33	0.0315	0.0159	93.08
0.15	0.21	0.33	0.0291	0.0171	92.66
0.25	0.20	0.33	0.0281	0.0169	92.96
0.35	-	0.32	-	0.0189	92.55
0.5	-	0.32	-	0.0170	92.98
0.6	-	0.31	-	0.0195	92.44
0.75	-	0.33	-	0.0164	92.89
0.9	-	0.33	-	0.0185	92.28
1	-	0.29	-	0.0181	93.54
Average	0.19 ± 0.03	0.33 ± 0.01	0.0297 ± 0.0005	0.0171 ± 0.0003	92.83 ± 0.07

As shown by Fig. 8 (and also Fig. 5), a power-law regime described by the exponent S_0 was identified. The extrapolation of the respective fitting to the temperature axis yields a precise value for $T_{C0}(H)$, defining the zero resistance state toward low temperatures. The exponent has an average value of 2.37 ± 0.03, as shown in the Table 4, where the values of T_{C0} and the respective amplitudes A_0 are also listed. This regime can be interpreted based on a paracoherent-coherent transition of a granular array, such as proposed by Rosenblatt.[23,36,37] In this case, according to the authors, during the paracoherent-coherent transition the order parameter in each superconducting grain achieves a long-range order due to the activation of the weak links among them. For granular superconductors, when the temperature is decreased below T_P the order parameter reaches the maximum amplitude inside the superconducting grains, although there are phase fluctuations. However, when the temperature is lowered the Josephson coupling energy among the superconducting grains may surpass the entropy, allowing the establishment of a long-range phase ordered state and signaling the coherence transition, used to describe the approach to the zero resistance state in polycrystalline materials.

Our results are similar to previous results obtained for Y123 samples in the approximation to zero resistance state,[15,38,39] and even in other superconducting cuprates.[40] However, our results differ from previous results obtained for Y358 samples.[13] Such difference is not surprising, once that similar behavior can be observed in Y123 samples, where the respective exponent may be found from 2.8 up to 4.0.[14,15,41]

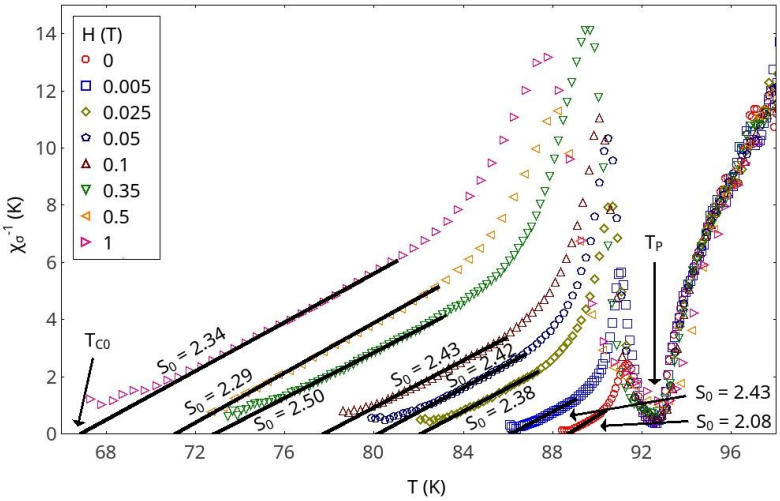

Fig. 8. Plots of χ^{-1} versus T showing the conductivity fluctuations near the zero resistance state, represented by the exponent S_0. T_P is indicated and T_{C0} defines the zero resistance state for each magnetic field (see Table 4).

Table 4. Results for fluctuations near the zero resistance state, represented by the exponent S_0. The reduced temperature ε, the temperature T_{C0} extrapolated from S_0, and the respective amplitude A_0 are also listed.

H (T)	S_0 $0.0018 \leq \varepsilon \leq 0.2242$	T_{C0}	A_0 $(m\Omega.cm)^{-1}$
0	2.08	88.69	0.00048
0.005	2.43	86.11	0.00063
0.025	2.42	82.09	0.00289
0.04	2.42	81.15	0.00386
0.05	2.38	80.16	0.00544
0.075	2.39	78.88	0.00717
0.1	2.43	77.75	0.00844
0.15	2.44	76.70	0.01037
0.25	2.46	74.07	0.01585
0.35	2.50	72.86	0.01799
0.5	2.29	71.11	0.03202
0.6	2.36	70.50	0.03608
0.75	2.32	68.70	0.04255
0.9	2.30	67.05	0.05410
1	2.34	66.97	0.06593
Average	2.37 ± 0.03		

4. Conclusion

We have performed an experimental study in a polycrystalline $Y_3Ba_5Cu_8O_{18}$ (Y358) sample, in order to investigate the superconducting transition focusing on the magnetoconductivity fluctuations. Magnetic fields up to 1 T were applied and the superconducting transition showed a two-step process, characteristic of a granular system governed by Josephson junctions strongly affected by the field. As a consequence, the temperature where the zero electric resistance is obtained was also seriously affected. However, the pairing critical temperature T_P, that denotes the superconductivity stabilization inside the grains, showed slightly affected by the magnetic field.

Above the pairing critical temperature two Gaussian regimes were observed, represented by the exponents $\lambda_{2D} = 0.98 \pm 0.02$ and $\lambda_{3D} = 0.51 \pm 0.01$, corresponding to 2D and 3D superconducting fluctuations respectively, and one regime corresponding to a fractal regime given by $\lambda_{3D\leftrightarrow 2D} = 0.74 \pm 0.05$. The 3D Gaussian regime showed a robustness for magnetic fields as high as 1 T, with no apparent tendency to be suppressed. This result is interesting and contrasts with previous results found in the Y358.

Still above the pairing critical temperature we observed an exponent given by $\lambda_C = 0.33 \pm 0.01$, corresponding to genuine critical fluctuations described by 3D-XY-E model. This regime also showed a robustness for magnetic fields up to 1 T, with no tendency of suppression. This result is not common in the Y123 superconductor, and we suggest that can be an indicative for a specific behavior of the Y358 superconductor.

Immediately above the pairing critical temperature we observe the existence of another critical regime, represented by the exponent $\lambda_{SC} = 0.19 \pm 0.03$ and persistent up to 0.25 T. Our interpretation is based on previous works where this result can be credited to a possible weakly first-order transition in superconducting cuprates. According to our knowledge this result constitutes one of the first observations of this asymptotic critical regime in the Y358 system, thus reinforcing the assumption of a possible general characteristic in superconducting cuprates. On the other hand, the respective regime seems to be more robust in the Y358 in relation to the Y123 superconductor.

Below the pairing critical temperature, near the zero resistance state, one fluctuation regime was observed, represented by the exponent $S_0 = 2.37 \pm 0.03$. The regime is interpreted based on the paracoherent-coherent transition of a granular array proposed by Rosenblatt. This results is similar to other superconducting cuprates, however its value is lower when compared with previous results obtained for Y358 samples.

Acknowledgements

We acknowledge the support of the HLD-HZDR, member of the European Magnetic Field Laboratory (EMFL).

4. References

1. J. G. Bednorz and K. A. Müller, *Zeitschrift für Phys. B* **64**, 189 (1986).
2. A. A. Aliabadi, Y.A. Farshchi and M. Akhavan, *Physica C* **469**, 2012 (2009).
3. S. Kutuk *et al.*, *J. Alloys Compd.* **650**, 159 (2015).
4. N. Akduran, *J. Low Temp. Phys.* **168**, 323 (2012).
5. F. T. Dias *et al.*, *J. of Phys.: Conf. Series* **568**, 022009 (2014).
6. A. O. Ayas *et al.*, *J. Supercond. Nov. Magn.* **24**, 2243 (2011).
7. S. Gholipour *et al.*, *J. Supercond. Nov. Magn.* **25**, 2253 (2012).
8. J. Konne *et al.*, *Supercond. Sci. Technol.* **25**, 115005 (2012).
9. P. Udomsamuthirun *et al.*, *J. Supercond. Nov. Magn.* **23**, 1377 (2010).
10. A. Esmaeili *et al.*, *Eur. Phys. J. B* **79**, 443 (2011).
11. D. A. L. Téllez, M. C. Báez and J. Roa-Rojas, *Mod. Phys. Lett. B* **26**, 1250067 (2012).
12. S. Bollat and S. Kutuk, *J. Supercond. Nov. Magn.* **25**, 731 (2012).
13. Y. Slimani *et al.*, *Mod. Phys. Lett. B* **29**, 1550227 (2015).
14. P. Pureur *et al.*, *Phys. Rev. B* **47**, 11420 (1993).
15. V. N. Vieira, P. Pureur and J. Schaf, *Phys. Rev. B* **66**, 224506 (2002).
16. F. T. Dias *et al.*, *Physica B* **404**, 3106 (2009).
17. M. Hikita and M. Suzuki, *Phys. Rev. B* **39**, 4756 (1989).
18. U. Welp *et al.*, *Phys. Rev. Lett.* **67**, 3180 (1991).
19. P. C. Hohenberg and B. I. Halperin, *Rev. Mod. Phys.* **49**, 435 (1977).
20. J. R. Rojas *et al.*, *Phys. Rev. B* **61**, 12457 (2000).
21. V. N. Vieira, J. P. da Silva and J. Schaf, *Phys. Rev. B* **64**, 094516 (2001).
22. W. T. B. Sousa *et al.*, *J. Supercond. Nov. Magn.* **23**, 1307 (2010).
23. P. Peyral *et al.*, *J. Less-Common Met.* **151**, 49 (1989).
24. P. Pureur *et al.*, *Physica C* **176**, 357 (1991).
25. L. G. Aslamazov and A. I. Larkin, *Sov. Phys. Solid State* **10**, 875 (1968).
26. K. Char and A. Kapitulnik, *Z. Phys. B* **72**, 253 (1988).
27. M. A. Gusmão and P. M. Mors, *Phys Rev. B* **42**, 10030 (1990).
28. C. J. Lobb, *Phys. Rev. B* **36**, 3930 (1987).
29. J. C. Le Guillou and J. Zinn-Justin, *Phys. Rev. B* **21**, 3976 (1980).
30. P. C. Hohenberg and B. I. Halperin, *Rev. Mod. Phys.* **49**, 435 (1977).
31. R. M. Costa *et al.*, *Solid State Commun.* **113**, 23 (2000).
32. R. M. Costa *et al.*, *Phys Rev. B* **64**, 214513 (2001).
33. F. T. Dias *et al.*, *J. of Phys.: Conf. Series* **200**, 012027 (2010).
34. V. N. Vieira *et al.*, *J. of Phys.: Conf. Series* **391**, 012140 (2012).
35. F. W. Fabris. J. Roa-Rojas and P. Pureur, *Physica C* **354**, 304 (2001).
36. C. Lebeau *et al.*, *Physica B* **152**, 100 (1988).
37. J. Rosenblatt *et al.*, *Rev. Phys. Appl.* **25**, 73 (1990).
38. P. Rodrigues Jr. *et al.*, *Mod. Phys. Lett. B* **22**, 1717 (2008).
39. L. F. Lopes *et al.*, *J. of Phys.: Conf. Series* **568**, 022013 (2014).
40. P. Rodrigues Jr., A. R. Jurelo and F. T. Dias, *Mod. Phys. Lett. B* **16**, 1115 (2002).
41. A. R. Jurelo *et al.*, *Physica C* **311**, 133 (1999).